

# Analysis of Mechanical and Thermal Properties of Components Produced by Additive Manufacturing

J. Lokesh<sup>1</sup> | Ch. Manoj<sup>1</sup> | P. Kowshik Satya Sai<sup>1</sup> | K. D. Pavan Kaylan<sup>1</sup> | N. Pallavi Senapti<sup>2</sup>

<sup>1</sup>Students of Mechanical Engineering Department, Nadimpalli Satyanarayana Raju Institute of Technology, (NSRIT), Autonomous, Visakhapatnam – 531173.

<sup>2</sup>Department of Mechanical Engineering Department, Nadimpalli Satyanarayana Raju Institute of Technology, (NSRIT), Autonomous, Visakhapatnam – 531173.

## Abstract

Additive manufacturing, specifically fused deposition modelling (FDM), has revolutionized the production of complex components by enabling precise control over design parameters such as infill density. This paper investigates the mechanical and thermal properties of components fabricated from polylactic acid (PLA), a widely used biodegradable thermoplastic, with infill densities varied at 25%, 50%, 75%, and 100%. The study aims to elucidate how infill density influences the performance of PLA components, providing insights for optimizing their use in engineering applications. Mechanical properties were assessed through compression tests conducted on cylindrical samples, measuring compressive strength, elastic modulus, and deformation behaviour. The tests revealed that higher infill densities significantly enhance mechanical performance, with 100% infill components exhibiting the highest compressive strength and stiffness, while 25% infill samples showed greater ductility but reduced load-bearing capacity. Components with higher infill density demonstrated improved thermal conductivity due to increased material continuity, facilitating better heat transfer. However, lower infill density samples exhibited reduced thermal stability, with noticeable deformation under prolonged exposure to heat. These results underscore the importance of infill density in applications requiring thermal management, such as heat sinks or enclosures. The study integrates mechanical and thermal data to provide a comprehensive understanding of PLA component behaviour under varying infill conditions. The findings contribute to advancing additive manufacturing practices, enabling the production of PLA-based components tailored to specific functional requirements in fields such as aerospace, automotive, and consumer goods, while promoting sustainable material use.

**Keywords:** Additive Manufacturing, Fused Deposition Modelling (FDM), Polylactic Acid (PLA), Infill Density, Compression Tests, Thermal Properties.

## 1. Introduction

Additive manufacturing (AM), commonly known as 3D printing, has emerged as a transformative technology in modern engineering, enabling the production of complex geometries with unprecedented design flexibility. Among AM techniques, fused deposition modelling (FDM) is widely adopted due to its cost-effectiveness, accessibility, and ability to process a variety of thermoplastic materials. Polylactic acid (PLA), a biodegradable and environmentally friendly polymer, is one of the most popular materials used in FDM, valued for its ease of printing, low processing temperature, and sustainability. However, the performance of PLA-based components, particularly their mechanical and thermal properties, is highly dependent on printing parameters, with infill density being a critical factor. This project focuses on analysing how infill density (25%, 50%, 75%, and 100%) affects the mechanical and thermal characteristics of PLA components produced via FDM, aiming to provide insights for optimizing their design and application.

Infill density, defined as the percentage of internal material fill within a printed component, directly influences material usage, weight, and performance. Lower infill densities reduce material consumption and production time, making it attractive for cost-sensitive applications, but it may compromise strength and durability. Conversely, higher infill density enhances structural integrity but increases resource demands. Understanding this trade-off is essential for tailoring components to specific requirements, such as load-bearing parts in automotive or aerospace industries or thermally stable enclosures in electronics. Mechanical properties, assessed through compression tests, reveal how infill density affects

compressive strength, stiffness, and deformation behaviour. Similarly, thermal tests evaluate thermal conductivity and stability, critical for applications involving heat exposure.

This study addresses the need for comprehensive data on PLA's behaviour under varying infill conditions, bridging the gap between design flexibility and functional performance. By systematically analysing the interplay between infill density, mechanical strength, and thermal efficiency, the project contributes to advancing additive manufacturing practices, enabling the production of optimized, sustainable PLA components for diverse engineering applications.

The motivation for this research stems from the growing adoption of additive manufacturing in both industrial and consumer applications, where PLA components are increasingly utilized for prototyping, functional parts, and sustainable product development. Despite PLA's widespread use, there remains a lack of detailed studies exploring the combined effects of infill density on both mechanical and thermal properties, particularly under standardized testing conditions. Compression tests in this project provide quantitative data on how infill density governs load-bearing capacity and failure modes, offering insights into the material's suitability for structural applications

Concurrently, thermal tests assess PLA's response to temperature variations, crucial for determining its performance in environments with heat exposure, such as electronic housings or automotive components. By varying infill density at 25%, 50%, 75%, and 100%, this study systematically investigates the balance between material efficiency and performance, addressing key challenges in achieving lightweight yet robust designs. The findings aim to guide engineers and designers in selecting optimal printing parameters, enhancing the reliability and functionality of PLA-based components while promoting resource-efficient manufacturing practices aligned with sustainability goals.

## 2. Materials and Methods

The objective of this study was to analyse the influence of infill density on the mechanical and thermal properties of polylactic acid (PLA) components produced via fused deposition modelling (FDM). Cylindrical test specimens (20 mm diameter, 40 mm height) were designed using CAD software and fabricated using a commercial FDM 3D printer with a 0.4 mm nozzle. PLA filament (1.75 mm diameter, density 1.24 g/cm<sup>3</sup>) was selected for its widespread use and sustainability. Four infill density levels—25%, 50%, 75%, and 100%—were chosen to represent a range of material fill configurations, with a rectilinear infill pattern to ensure consistency. Printing parameters were standardized: layer height of 0.2 mm, print speed of 50 mm/s, nozzle temperature of 200°C, and bed temperature of 60°C. Four specimens per infill density were printed to account for variability, resulting in 16 total samples for mechanical testing and 16 for thermal testing.



Fig. 1. 3D Printing Machine and samples produced

### 2.1 Compression Testing

Compression tests were conducted using a universal testing machine (UTM) with a 50 KN load cell, following ASME standards for compressive properties of rigid plastics. Specimens were placed centrally between parallel platens, and a

constant crosshead speed of 1.3 mm/min was applied until failure or significant deformation occurred. Load-displacement data were recorded to calculate compressive strength (maximum stress), elastic modulus (initial linear slope of stress-strain curve), and deformation behaviour. Tests were performed at ambient conditions to ensure repeatability.



Fig. 2 Compression testing in INSTRON Machine

### **2.2 Thermal Testing**

Thermal properties were evaluated using a guarded hot plate apparatus to measure thermal conductivity and a thermogravimetric analyser (TGA) to assess thermal stability. For thermal conductivity, specimens were subjected to a steady-state heat flow at 50°C, with temperature sensors recording the gradient across the sample thickness. Thermal conductivity ( $k$ ) was calculated using Fourier's law. For thermal stability, TGA was conducted from 25°C to 400°C at a heating rate of 10°C/min under a nitrogen atmosphere to determine the onset of thermal degradation and mass loss. Tests were repeated 5 times per infill density to ensure statistical reliability.



Fig. 3 Thermal conductivity test

### **2.3 Mechanical Properties of PLA Components**

The mechanical properties of polylactic acid (PLA) components produced through additive manufacturing play a crucial role in determining their applicability across various industries. The performance of Fused Deposition Modelling (FDM) printed PLA is significantly influenced by several printing parameters such as layer thickness, nozzle temperature, and print speed, which can affect tensile strength, yield strength, and elasticity. Notably, research has demonstrated that optimal settings can yield a maximum ultimate tensile strength (UTS) of 40.68 MPa under conditions of 0.2 mm layer thickness, 220°C nozzle temperature, and a print speed of 120 mm/s, showcasing the materials potential for structural applications (Islam et al.). Furthermore, the layer-by-layer manufacturing process in FDM contributes to a unique fatigue behavior that necessitates careful analysis to understand how it compares with traditionally manufactured polymers (Babu K et al.). Thus, a thorough investigation into these mechanical properties is essential for enhancing the reliability and performance of PLA components in practical applications.

**2.4 Impact of Infill Density on Compression Strength and Durability**

Understanding the impact of infill density on the compression strength and durability of components fabricated through additive manufacturing is crucial for optimizing their performance in practical applications. Variations in infill density directly influence the mechanical integrity of printed parts, particularly when using materials such as polylactic acid (PLA). Higher infill densities typically enhance compression strength by providing greater material support and reducing voids within the structure, ultimately leading to improved durability. However, this increase in strength can come at the expense of weight and material efficiency, an important consideration in applications demanding lightweight components. As noted, the mechanical behavior of FDM printed polymers can be complex due to layer adhesion imperfections and anisotropic characteristics inherent in the manufacturing process (Babu K et al.). Moreover, the lack of standardized testing methods further complicates the assessment of these materials’ performance, revealing critical gaps in our understanding of the interplay between infill density and overall mechanical properties

**2.5 Thermal Properties of PLA Components**

The thermal properties of Polylactic Acid (PLA) components are crucial for assessing their performance in additive manufacturing applications, particularly under varying operational conditions. PLA exhibits a relatively low glass transition temperature and melting temperature, which influences its dimensional stability and mechanical integrity when subjected to heat. As demonstrated in studies, the thermal behavior of PLA can be significantly affected by processing parameters such as layer thickness and nozzle temperature, underscoring the complexity of Fused Deposition Modeling (FDM) techniques. For instance, variations in nozzle temperature directly impact the ultimate tensile strength (UTS) and Youngs modulus of the printed material, revealing the importance of optimizing printing parameters to enhance thermal performance (Islam et al.). Moreover, understanding the thermal properties is critical for applications that demand consistent performance under thermal stress, as highlighted by the insights gathered through thermal analysis within the context of ASME standards.

**3. Results and discussion:**

In the present work, ABS specimens were 3D printed by FDM process by varying the lattice structure and cell size. Total 9 lattice structures were used and 3 cell sizes were adopted. The specimens were tested for strength, surface roughness and thermal conductivity and the results were presented and discussed in this section.

The densities were calculated for all specimens and the data is presented in Table 2. From these values it is observed that the density of 3D printed specimens with Minimal surface with Diamond Minimal Surface lattice structure is more compared to other lattice structures. It is evident from Fig. 1 that the lattice structure “Minimal surface with Diamond Minimal Surface” is closely packed and hence resulted in more density after 3D print.

**Table 1** Densities of specimens printed with various Lattice Structures and cell sizes

Specimen No.	Name of the lattice structures	Density(g/cm <sup>3</sup> )		
		Unit cell size (4)	Unit cell size(5)	Unit cell size (6)
1.	Cubit truss structure with inner truss beams	0.4916	0.3591	0.2915
2.	Cubic Truss Structure with outer, inner horizontal and diagonal truss beams	0.50624	0.3022	0.3009

3.	Quasi-Radial truss with Inner truss structure	0.6260	0.3811	0.3042
4.	Herring Bone structure with Triangular outer truss and inner truss structure	0.5318	0.4181	0.3153
5.	Octagonal Truss structure	0.2986	0.2854	0.2775
6.	Triangular truss structure with inner truss beams	0.5351	0.4183	0.3182
7.	Gyroid Minimal Surface	0.6115	0.5427	0.5460
8.	Primitive Minimal Surface	0.5253	0.5120	0.4791
9.	Minimal surface with Diamond Minimal Surface	0.6897	0.6683	0.6275

The bending test results were presented in Table 2. The results of bending test were also represented in the graph (Fig. 8 and 9). Based on the bending strength values obtained for unit cell size 5 specimens, we have chosen only 4 specimens for bending test with cell size 4 and 6. From these results it is observed that flexural strength is more in specimen number 7 (Gyroid Minimal Surface) with unit cell size 4 (36.98157MPa) followed by specimen number 9 (Minimal surface with Diamond Minimal Surface) with unit cell size 5 (35.57466 MPa) and specimen number 8 (Primitive Minimal Surface) with unit cell size 5 (28.11407 MPa). This observation reveals that the flexural strength of 3D printed ABS material specimens with minimal surface structures is better compared to other type of structures.

**Table 2** Flexural strength of specimens 3D printed with various lattice structures and cell sizes

Specimen No.	Lattice structures	Unit cell size =4		Unit cell size =5		Unit cell size =6	
		Flexural strength at maximum flexure load (MPa)	Flexural modulus (GPa)	Flexural strength at maximum flexure load (MPa)	Flexural modulus (GPa)	Flexural strength at maximum flexure load (MPa)	Flexural modulus (GPa)
1.	Cubit truss structure with inner truss beams			13.846	0.438		
2.	Cubic Truss Structure with outer, inner horizontal and Diagonal truss beams	16.16	0.584	13.248	0.413	11.914	0.451

3.	Quasi-Radial truss with Inner truss structure			14.375	0.470		
4.	Herring Bone structure with Triangular outer truss and inner truss structure	18.243	0.620	12.600	0.474	12.733	0.466
5.	Octagonal Truss structure			9.817	0.414		
6.	Triangular truss structure with inner truss beams			15.128	0.464		
7.	Gyroid Minimal Surface	36.981	1.2631	25.101	0.712	23.252	0.733
8.	Primitive Minimal Surface			28.114	0.795		
9.	Minimal surface with Diamond Minimal Surface	28.754	1.1253	35.574	0.916	27.189	0.982

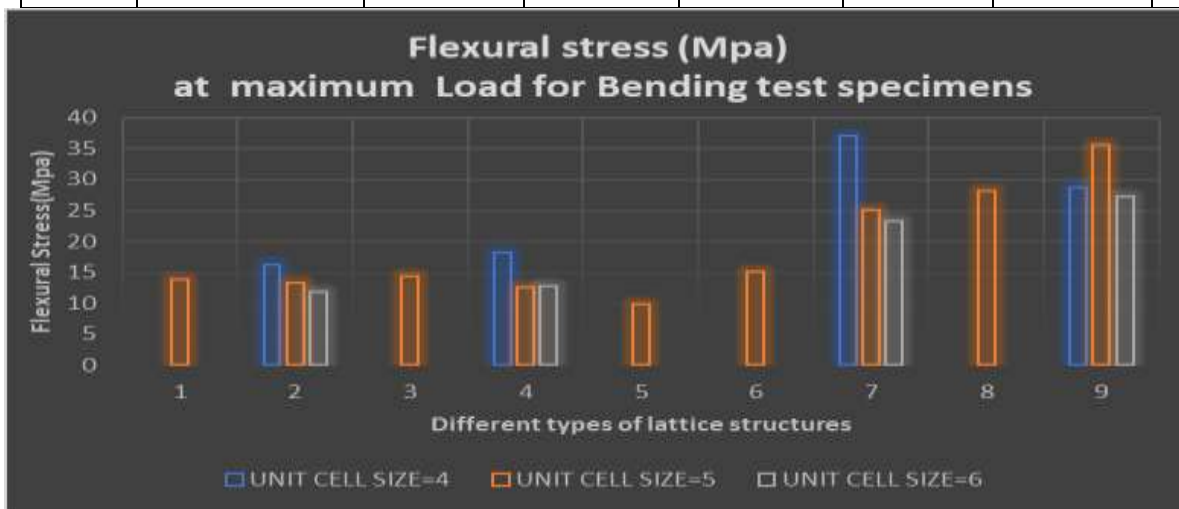


**Fig. 4** Graphical representation of flexural strength values of 3D printed specimen with various lattice structures and three different unit cell sizes

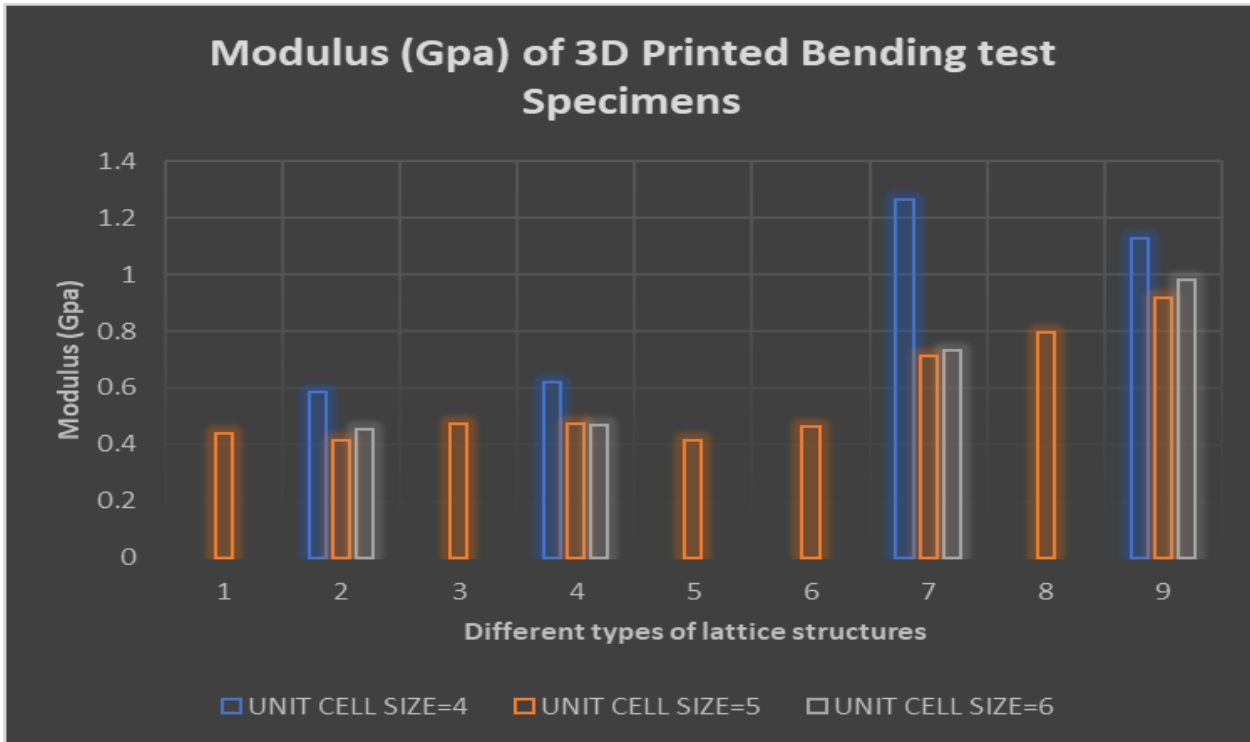


**Fig. 5** The graph showing the variations in flexural modulus of different unit cell sizes and with various lattice structures.

The compression test results were presented in Table 4. The results of bending test were also represented in the graph (Fig. 10 and 11). Based on the compression strength values obtained for unit cell size 5 specimens, we have chosen only 4 specimens for compression test with cell size 4 and 6. From these results it is observed that compression strength is more in specimen number 7 (Gyroid Minimal Surface) with unit cell size 4 (19.83 MPa) followed by specimen number 9 (Minimal surface with Diamond Minimal Surface) with unit cell size 4 (18.71 MPa) and specimen number 8 (Primitive Minimal Surface) with unit cell size 5 (10.27 MPa). This observation reveals that the compression strength of 3D printed ABS material specimens with minimal surface structures is better compared to other type of structures. The similar phenomenon was observed with the compression modulus values also.

**Table 3:-**Compression test results of specimens with different lattice structures and unit cell sizes.

Specimen No.	LATTICE STRUCTURES	UNIT CELL SIZE =4		UNIT CELL SIZE =5		UNIT CELL SIZE =6	
		Compressive Strength (MPa)	Modulus (GPa)	Compressive Strength (MPa)	Modulus (GPa)	Compressive Strength (MPa)	Modulus (GPa)
1.	Cubit truss structure with inner truss beams			6.09	0.2018		

2.	Cubic Truss Structure with outer, inner horizontal and diagonal truss beams	16.07	0.47406	1	0.07709	3.28	0.18269
3.	Quasi-Radial truss with Inner truss structure			8.66	0.27722		
4.	Herring Bone structure with Triangular outer truss and inner	12.26	0.38889	8.33	0.27335	3.66	0.17013

	truss structure						
5.	Octagonal Truss structure			1.94	0.08985		
6.	Triangular truss structure with inner truss beams			8.27	0.29897		
7.	Gyroid Minimal Surface	19.83	0.6098	13.74	0.39871	19.6	0.21292
8.	Primitive Minimal Surface			10.27	0.32132		
9.	Minimal surface with Diamond Minimal Surface	18.71	0.550980	18.45	0.5095	18.31	0.4586

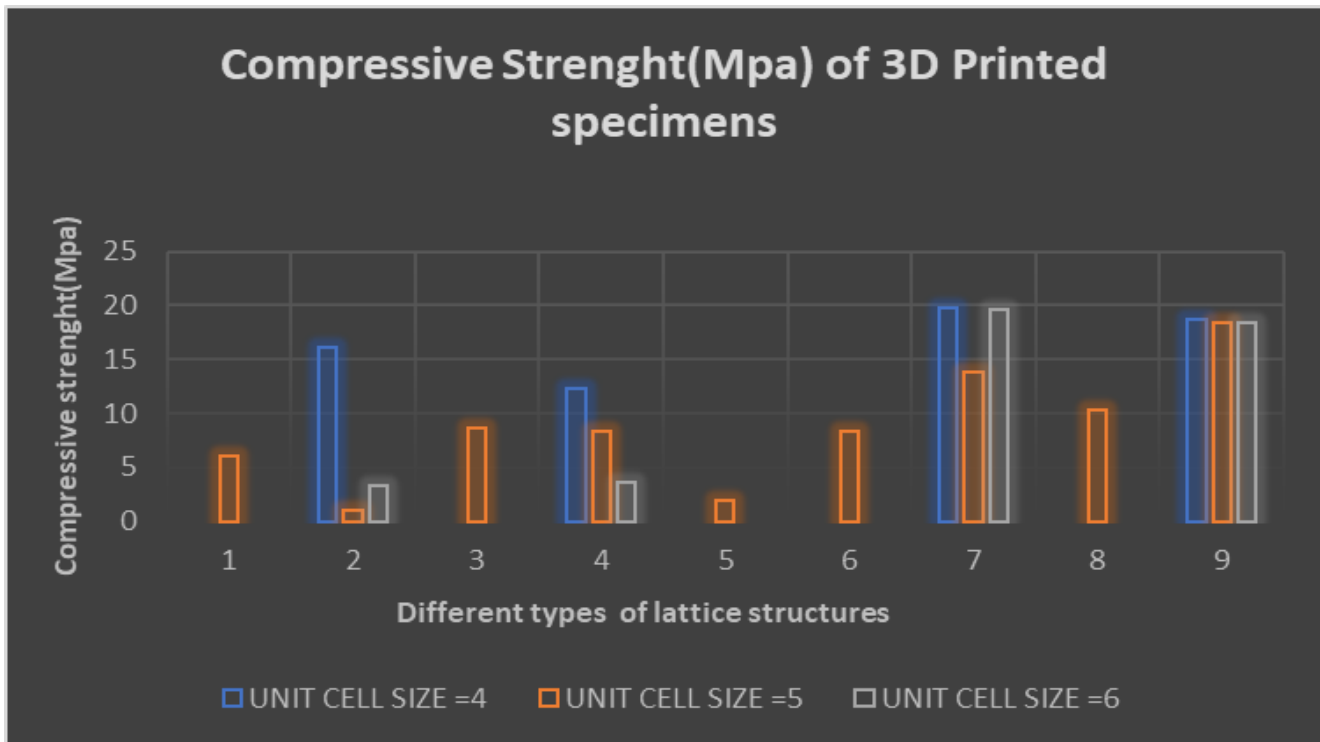


**Fig. 6** The chart demonstrates differences in three distinct unit cell sizes of compressive strength for the compressive test as well as between several lattice structures.

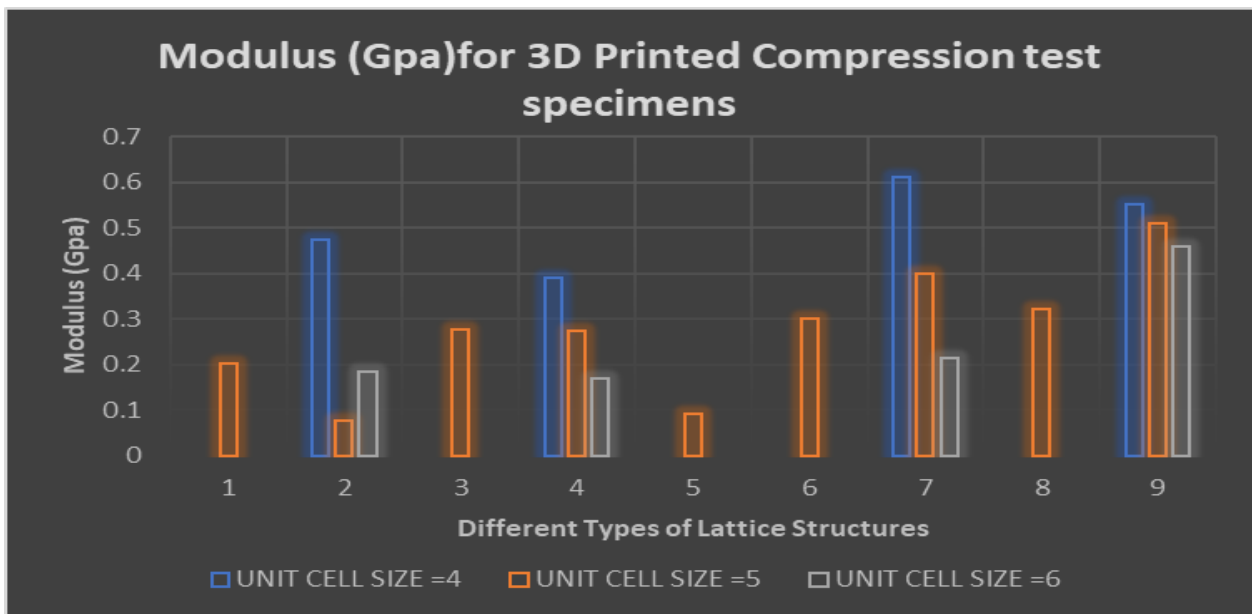


**Fig. 7** The graph showing the compression modulus (GPa) of three distinct unit cell sizes from the compressive test with several lattice structures.

To study the effect of lattice structure on surface roughness of the 3D printed specimen, surface roughness measurement was carried out on the 9 specimens. The results of the surface roughness test were presented in Table 5 and the values were represented graphically in Fig. 12. From these values it is observed that the surface roughness value is minimum for specimen number 1 (Cubit truss structure with inner truss beams) lattice structure i.e. (1.7495  $\mu\text{m}$ ).

**Table 4** Surface roughness ( $\mu\text{m}$ ) values for nine different lattice structures

Specimen No.	NAMES OF LATTICE STRUCTURES	Surface roughness ( $\mu\text{m}$ )	
		Rax (Avg)	Ray (Avg)
1	Cubit truss structure with inner truss beams	1.7495	5.988
2	Cubic Truss Structure with outer, inner horizontal and diagonal truss beams	1.87	9.405
3	Quasi-Radial truss with Inner truss structure	2.126	8.672
4	Herring Bone structure with	2.987	10.308
	Triangular outer truss and inner truss structure		
5	Octagonal Truss structure	2.243	8.418
6	Triangular truss structure with inner truss beams	2.327	5.347
7	Gyroid Minimal Surface	3.755	4.7005
8	Primitive Minimal Surface	2.633	5.598
9	Minimal surface with Diamond Minimal Surface	1.919	7.0495

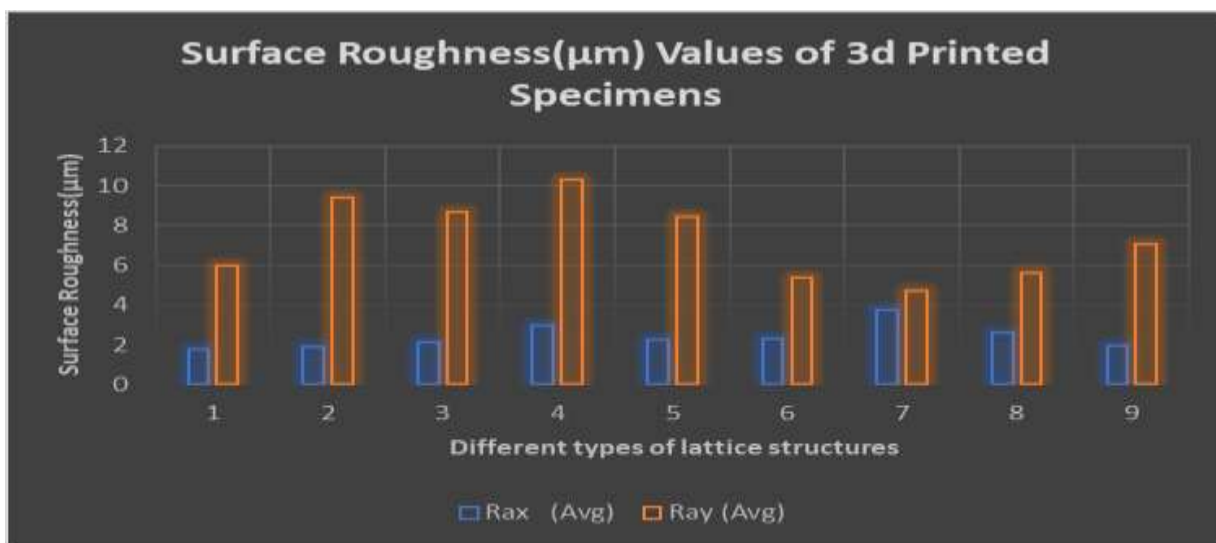


**Fig. 8** Graphical representation of surface roughness results for nine lattice structures.

The thermal conductivity test results were presented in Table 6. The results of thermal conductivity test were also represented in the graph (Fig. 13). As a rule of thumb, the lower the thermal conductivity the better, because the material conducts less heat energy. Based on the thermal conductivity values obtained for unit cell size 5 specimens, we have chosen only 4 specimens for compression test with cell size 4 and 6. From these results it is observed that the thermal conductivity is less in specimen number 2 (Cubic Truss Structure with outer, inner horizontal and diagonal truss beams) with unit cell size 6 (0.2503 W/mK) followed by specimen number 9 (Minimal surface with Diamond Minimal Surface) with unit cell size 4 (0.2599 W/mK) This observation reveals that the thermal conductivity of 3D printed ABS material specimens with Cubic Truss Structure with outer, inner horizontal and diagonal truss beams and minimal surface structure is minimum compared to other type of structures.

**Table 5** Thermal conductivity ((W/mK) of 3D printed specimens with different lattice structures and unit cell sizes

Sample No.	Names of Different Lattice Structures	Thermal Conductivity (W/mK)		
		UNIT CELL SIZE =4	UNIT CELL SIZE =5	UNIT CELL SIZE =6
1	Cubit truss structure with inner truss beams		0.4165	
2	Cubic Truss Structure with outer, inner horizontal and diagonal truss beams	0.8888	0.2503	0.7505
3	Quasi-Radial truss with Inner truss structure		0.2642	
4	Herring Bone structure with Triangular outer truss and inner truss structure	1.0964	0.4905	0.4778
5	Octagonal Truss structure		0.4840	
6	Triangular truss structure with inner truss beams		0.3519	
7	Gyroid Minimal Surface	0.8022	0.4019	0.6397
8	Primitive Minimal Surface		0.4744	
9	Minimal surface with Diamond Minimal Surface	0.2599	0.4162	0.8116

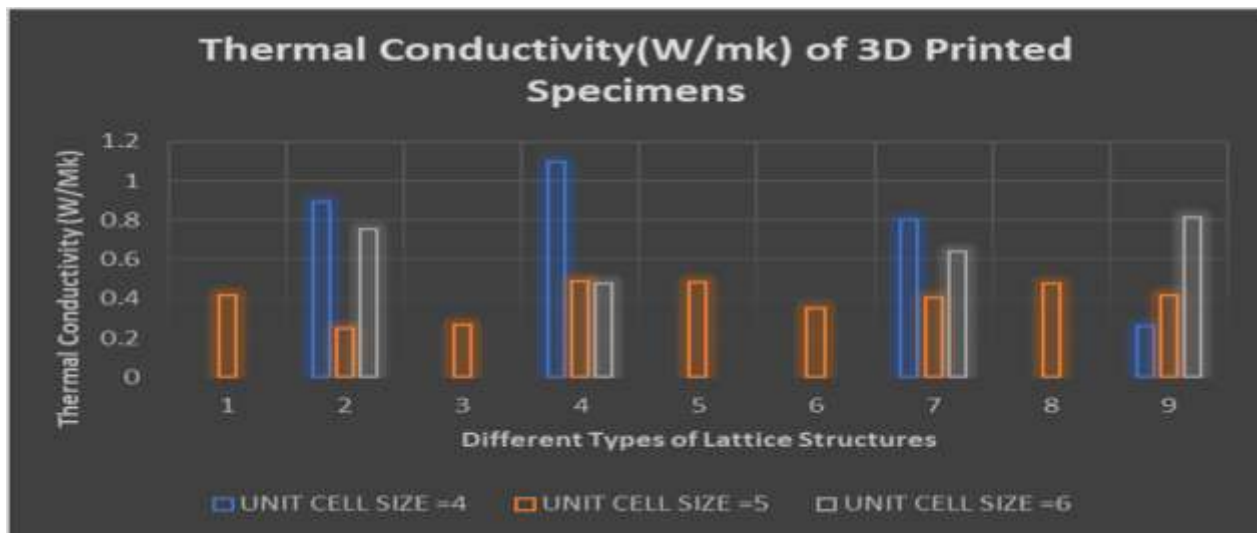


**Fig. 9** Graph showing the results of thermal Conductivity of nine lattice structures and three unit cell sizes,

#### 4. Conclusion

(i) Densities of 3D Printed Specimens: The measurement of densities provides insight into how different lattice structures and unit cell sizes affect the packing density of the ABS material. The observation that the "Minimal surface with Diamond Minimal Surface" lattice structure resulted in higher density indicates that this particular lattice configuration allows for more efficient material packing, likely due to its geometric characteristics.

(ii) Flexural Strength and Modulus: Flexural strength refers to a material's ability to resist deformation under bending forces, while flexural modulus indicates its stiffness. The finding that 3D printed ABS specimens with minimal surface structures exhibited superior flexural strength and modulus compared to other lattice structures suggests that these lattice configurations provide enhanced mechanical performance against bending stresses.

(iii) Compression Strength and Modulus: Compression strength measures a material's ability to withstand loads applied in a compression direction, while compression modulus represents its resistance to deformation under compressive loads. The observation that 3D printed ABS specimens with minimal surface structures displayed higher compression strength and modulus implies that these lattice configurations offer better resistance to compression forces and reduced deformation under compression.

(iv) Surface Roughness: Surface roughness refers to the irregularities or texture variations on the surface of a material. The result indicating that the surface roughness value was lowest for the lattice structure of specimen number 1 (Cubit truss structure with inner truss beams) suggests that this particular lattice configuration yields a smoother surface finish. The observed minimum thermal conductivity in ABS specimens with "Cubic Truss Structure" suggests its higher porosity, hindering heat transfer. Similarly, the intricate geometry of "Minimal Surface with Diamond Minimal Surface" limits heat conduction. These properties make them ideal for applications requiring effective thermal insulation. Understanding such characteristics aids in optimizing material selection for diverse engineering needs.

#### References

[1] Pentek, A., Nyitrai, M., Schiffer, A., Abraham, H., Bene, M., Molnar, E., Told, R. & Maroti, P. (2020). "The Effect of Printing Parameters on Electrical Conductivity and Mechanical Properties of PLA and ABS Based Carbon Composites in Additive Manufacturing of Upper Limb Prosthetics." *Crystals*, 10, 398. DOI: <https://doi.org/10.3390/cryst10050398>

[2] Maier, R., Istrate, A.M., Despa, A., Mandoc, A.C., Bucaciuc, S., & Stoica, R. (2022). "Investigation into Thermomechanical Response of Polymer Composite Materials Produced through Additive Manufacturing Technologies." *Materials*, 15, 5069. DOI: <https://doi.org/10.3390/ma15145069>

[3] Ivorra-Martinez, J., Quiles-Carrillo, L., Lascano, D., Ferrandiz, S., & Boronat, T. (2020). "Effect of infill parameters on mechanical properties in additive manufacturing." *Dyna*, 95(4), 412-417. DOI: <http://dx.doi.org/10.6036/9674>

- [4] Kumar, R., Chohan, J.S., Kumar, R., Yadav, A., Piyush, & Kumar, P. (2020). "Metal spray layered hybrid additive manufacturing of PLA composite structures: Mechanical, thermal and morphological properties." *Journal of Thermoplastic Composite Materials*, XX(X), 1-21. DOI: <https://doi.org/10.1177/0892705720932622>
- [5] Laureto, J., Tomasi, J., King, J.A., & Pearce, J.M. (2017). "Thermal properties of 3-D printed polylactic acid-metal composites." *Progress in Additive Manufacturing*, 2, 57-71. DOI: <https://doi.org/10.1007/s40964-017-0019-x>
- [6] Lendvai, L., Fekete, I., Rigotti, D., & Pegoretti, A. (2025). "Experimental study on the effect of filament-extrusion rate on the structural, mechanical and thermal properties of material extrusion 3D-printed polylactic acid (PLA) products." *Progress in Additive Manufacturing*, 10, 619-629. DOI: <https://doi.org/10.1007/s40964-024-00646-5>
- [7] Sehhat, M.H., Mahdianikhotbesara, A., & Yadegari, F. (2022). "Impact of Temperature and Material Variation on Mechanical Properties of Parts Fabricated with Fused Deposition Modelling (FDM) Additive Manufacturing." *Research Square*. DOI: <https://doi.org/10.21203/rs.3.rs-1079840/v2>
- [8] Caminero, M.Á., Chacón, J.M., García-Plaza, E., Núñez, P.J., Reverte, J.M., & Becar, J.P. (2019). "Additive Manufacturing of PLA-Based Composites Using Fused Filament Fabrication: Effect of Graphene Nanoplatelet Reinforcement on Mechanical Properties, Dimensional Accuracy and Texture." *Polymers*, 11, 799. DOI: <https://doi.org/10.3390/polym11050799>
- [9] Mohammadizadeh, M., Lu, H., Fidan, I., Tantawi, K., Gupta, A., Hasanov, S., Zhang, Z., Alifui-Segbaya, F., & Rennie, A. (2020). Mechanical and Thermal Analyses of Metal-PLA Components Fabricated by Metal Material Extrusion. *Inventions*, 5, 44. DOI: <https://doi.org/10.3390/inventions5030044>
- [10] Johnston, R., & Kazancı, Z. (2021). Analysis of additively manufactured (3D printed) dual-material auxetic structures under compression. *Additive Manufacturing*, 38, 101783. DOI: <https://doi.org/10.1016/j.addma.2020.101783>
- [11] Primo, T., Calabrese, M., Del Prete, A., & Anglani, A. (2017). Additive manufacturing integration with topology optimization methodology for innovative product design. *The International Journal of Advanced Manufacturing Technology*, 93, 467–479. DOI: <https://doi.org/10.1007/s00170-017-0112-9>
- [12] Ahmed, A., & Ali, M. (2020). "Experimental Analysis of Cryogenic Treatment on 3D Printed ABS Parts." *Materials Science and Engineering: A*, 796, 140060. DOI: <https://doi.org/10.1016/j.msea.2020.140060>
- [13] Sun, W., & Li, X. (2018). "Cryogenic Treatment of Additively Manufactured Ti-6Al-4V: Effects on Microstructure and Mechanical Properties." *Journal of Alloys and Compounds*, 766, 785-792. DOI: <https://doi.org/10.1016/j.jallcom.2018.06.182>
- [14] Wang, Y., & Jiang, P. (2021). "Cryogenic Treatment in Additive Manufacturing: Influence on the Fatigue Performance of Metal Parts." *International Journal of Fatigue*, 153, 106457. DOI: <https://doi.org/10.1016/j.ijfatigue.2021.106457>
- [15] Kumar, P., & Singh, R. (2022). "Impact of Cryogenic Treatment on Wear and Tensile Properties of 3D Printed AlSi10Mg Alloy." *Materials Letters*, 307, 131012. DOI: <https://doi.org/10.1016/j.matlet.2021.131012>
- [16] Gupta, S., & Kapoor, A. (2019). "Cryogenic Treatment Effects on the Durability of 3D Printed Composite Structures." *Journal of Composite Materials*, 53(5), 635-648. DOI: <https://doi.org/10.1177/0021998318796368>